

Chapter Number

Atmospheric corrosion studies in a decommissioned nuclear power plant

Manuel Morcillo, Eduardo Otero, Belén Chico and Daniel de la Fuente
Centro Nacional de Investigaciones Metalúrgicas (CENIM-CSIC)
Spain

1. Introduction

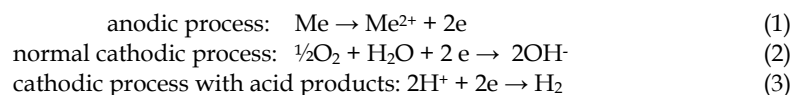
1.1. Fundamentals of the atmospheric corrosion of metals

Metallic corrosion progresses at a very low rate at room temperature in a perfectly dry atmosphere and for practical purposes may be ignored, but on humid surfaces is a very relevant phenomenon. The mechanism is electrochemical, with an electrolyte constituted by an extremely thin moisture film of just a few monolayers or an aqueous film of hundreds of microns in thickness due, for instance, to rain or dew (Rozenfeld, 1972; Barton, 1976; Feliu & Morcillo, 1982; Kucera & Mattson, 1986; Costa et al., 2006).

A considerable part of the damage that atmospheric corrosion causes to structures and equipment may be attributed to the condensation of humidity as a result of periodic cooling of the air. The formation of dew depends on the relative humidity (RH) of the air and the change in the metal surface temperature. The drier the atmosphere, the more the temperature must fall in order for humidity to condense; while at high RH a slight drop in temperature can lead to the saturation in humidity of the atmosphere. The fraction of time in which an atmosphere presents a high RH level has been shown to be a good indicator of its potential aggressivity.

Even in non-saturated atmospheres, where the formation of dew is theoretically not possible, water vapour may condense as a result of capillary and chemical condensation phenomena. Capillary condensation is favoured by rough surfaces, surfaces covered with porous corrosion products, and surfaces upon which dust has been deposited. Chemical condensation is due to the hygroscopic properties of certain polluting substances deposited on the metal surface, or the corrosion products themselves.

The corrosion reaction rate rises with the concentration of substances capable of ionising in the moisture film. Under this film the metal corrodes due to the cathodic process of reduction of oxygen from the air. Hydrogen ion discharging is only a relevant reaction when there is a high degree of pollution by acid products. Anodic corrosion of the metal (*Me*), when bivalent, and the aforementioned cathodic processes may be expressed in simplified terms by the reactions:



1.1.1. Time of wetness of the metallic surface

The atmospheric corrosion process is the sum of the partial (individual) corrosion processes that take place every time an electrolyte layer forms on the metal. Aqueous precipitation (rain, snow or fog) and the condensation of humidity due to temperature changes are, without doubt, the main promoters of atmospheric corrosion; if τ_i is the duration of each individual period of surface wetting and v_i is the mean corrosion rate in that period, the total corrosion after n periods will be:

$$c = \sum_{i=1}^n v_i \tau_i \quad (4)$$

τ_i includes both times of high RH and times of precipitation by rain, mist, fog, etc. v_i can vary greatly depending on the specific circumstances created by the different possible degrees of surface wetting and atmospheric pollution.

The sum of the partial times of surface wetting $\tau = \sum_{i=1}^n \tau_i$ constitutes what is known as the time of wetness (TOW), during which metallic corrosion is possible. Good correlation has been found between the TOW and the time during which RH exceeds a certain humidity level, generally above 70% (Rozenfeld, 1972; Barton, 1976).

1.1.2. Atmospheric pollution

As has been noted, corrosion is not likely below a certain RH level, due to the lack of an appreciable electrolyte film on the metal surface. The corrosion of iron and other metals is generally insignificant at a RH below 60-80%. Even when the RH exceeds this value, for the corrosion rate to be really considerable the atmosphere must also be polluted.

Of all atmospheric pollutants, NaCl and SO₂ are the commonest airborne corrosive agents. NaCl is incorporated in the atmosphere from the sea, and its strongest effects are seen close to the shoreline, where the air carries large amounts of salt and pulverised seawater. SO₂ of anthropic origin can reach considerable concentrations in atmospheres close to thermal power plants or otherwise polluted by smoke from industrial, domestic or transport-related sources. It is originated by burning fuels that contain sulphur.

These two chemical substances, NaCl and SO₂, greatly stimulate the corrosion of wetted metallic surfaces since they raise the activity of the aqueous film. For this reason, atmospheric corrosion in areas close to the sea usually considerably exceed what is expectable in unpolluted inland areas. The same goes for SO₂ emission sources, in whose

surroundings corrosion processes are accelerated. Numerous experimental studies have been carried out to quantify the relationship between corrosion rates and atmospheric SO₂ levels, and abundant information is available in the literature.

Quantitative information on chlorides is somewhat scarcer. Nevertheless, it has been perfectly established that chloride pollution plays an important role when its concentration exceeds certain levels.

1.1.3. Indoor atmospheric corrosion

Indoor atmospheric corrosion is a particular case of atmospheric corrosion experienced by metals exposed to the atmosphere in an enclosed environment (Leygraf & Graedel, 2000).

The factors influencing metal corrosion in indoor environments are basically the same as in outdoor exposure, although the atmospheric parameters can be very different (Chawla & Payer, 1991).

In outdoor environments, water interacts with the surface of materials in the form of adsorbed moisture, condensed water and direct precipitation. Indoors, the only relevant components in the formation of wetted surfaces are water and pollutants adsorbed from the atmosphere. Condensation is possible indoors, but requires an unusual combination of external weather conditions and indoor environmental conditions. This can be the case in warm, humid climates, and even in air-conditioned buildings, where water sometimes condenses on surfaces that are cooled below the dew point. Condensation may be capillary (favoured by the deposition of dust or the presence of corrosion products) or chemical (due to the hygroscopicity of these products). The levels of suspended solids and gaseous atmospheric pollutants are usually considerably lower indoors than outdoors.

The absence of visible aqueous films in indoor atmospheres and the much lower levels of the agents that favour chemical and capillary condensation make it more difficult for the electrolyte layer necessary for the development of electrochemical corrosion processes to form. The lower concentration of gaseous pollutants is another reason why metallic corrosion is notably lower in indoor environments (Chawla & Payer, 1991).

1.2. Corrosion studies in the decommissioned Vandellós I nuclear power plant

Vandellós I is a graphite-moderated, gas-cooled nuclear power plant of 497 MW capacity located in the province of Tarragona, Spain. It is the first nuclear power plant in Spain to be decommissioned. The decommissioning and dismantling plan is being coordinated by the National Radioactive Waste Management Company (ENRESA, Madrid, Spain).

Level 2 of the process, according to the International Atomic Energy Agency (IAEA, Vienna, Austria) nomenclature, was completed in 2002. The present step is a 30-year waiting period known as latency, whose purpose is to allow radiation inside the reactor containment vessel to fall to levels that permit its complete dismantling with a minimal radiological impact, in order to return the site to its original state. Thus it is necessary to guarantee the

containment's integrity during this time by assessing the possible risk of corrosion of the complex metallic structures located in its interior.

For this reason, besides determining the outdoor atmospheric corrosivity of the power plant site and constantly monitoring the temperature and relative humidity inside the reactor containment, ENRESA is monitoring the corrosivity of this indoor atmosphere to different types of structural steels.

This chapter describes the methodology followed to evaluate outdoor atmospheric corrosion at the power plant site and indoor atmospheric corrosion inside the concrete reactor containment during the latency period of decommissioning. Outdoor and indoor atmospheric corrosion rate results are also reported.

2. Outdoor atmospheric corrosion at the nuclear power plant site

Vandellós I nuclear power plant is located in an area where previous studies have indicated an atmosphere polluted only by sea salinity (pure marine atmosphere) and the practical absence of any other pollutants that can influence metallic corrosion processes (SO_2 , NO_x , etc.).

Atmospheric salinity is a parameter related with the amount of marine aerosol present in the atmosphere. Saline particles in marine atmospheres accelerate metallic corrosion processes because chlorides give rise to soluble corrosion products, in contrast to the scarcely soluble products that form in rural atmospheres. Dissolved marine chlorides also considerably raise the conductivity of the electrolyte layer on the metal surface and tend to destroy any existing passivating film.

Salinity in marine atmospheres varies within very broad limits (Bonnarens & Bragard, 1981; ISO 9223, 1992; Johnson & Stanners, 1981). While extremely high values have been recorded close to breaking waves, salinity at other points on the shoreline with calmer waters is more moderate.

The marine aerosol concentration decreases with altitude (Blanchard & Woodcock, 1980; Strekalov & Panchenko, 1994; Lovett, 1978). For this reason, raising a metal above ground level generally results in less corrosion as the number of saline particles reaching its surface decreases.

Despite the vast volume of information in the literature concerning the corrosion of metals in marine atmospheres, quantitative information on the effect of salinity on atmospheric corrosion is very scarce. Papers on this subject often make reference to a study carried out more than 50 years ago in Nigeria by Ambler and Bain (Ambler & Bain, 1955). The authors of this chapter have discussed the relationship between salinity and steel corrosion based on published data referring to research performed in different parts of the world (Morcillo et al., 1999) (Figure 1). Salinity values up to $100 \text{ mg Cl}^-/\text{m}^2\cdot\text{day}$ promote only a slight increase in the steel atmospheric corrosion rate, which becomes faster as the salinity rises up

to 400 mg Cl⁻/m².day. After this point the increase in corrosion with salinity is once again only slight, and subsequently seems to stabilise for higher atmospheric salinity values.

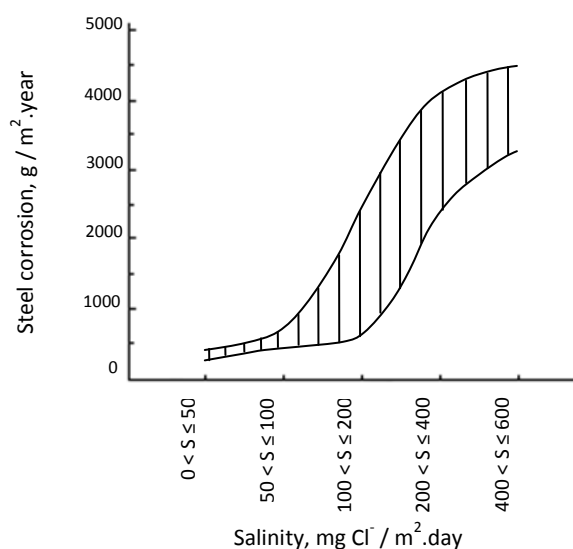


Fig. 1. Relation between salinity and steel corrosion (Morcillo et al., 1999)

The wind, which stirs up and transports particles of sea water, is the force responsible for the salinity present in marine atmospheres. Oceanic air is rich in marine aerosols resulting from the evaporation of drops of sea water that are mechanically transported by the wind. The origin, concentration and vertical distribution of marine aerosol over the surface of the sea has been studied by Blanchard and Woodcock (Blanchard & Woodcock, 1980).

Marine aerosol is composed of fine solid or liquid particles suspended in the air (jet drops, film drops, brine drops and sea-salt particles) of sizes of between 0.1 and 400 µm (Blanchard & Woodcock, 1980; Zezza & Macri, 1995). In marine atmospheres the aerosol concentration varies according to the altitude and wind speed.

The larger marine aerosol particles (diameter >10 µm), known as falling particles, remain in the atmosphere for only a short time; the greater the particle size, the shorter the time. In contrast, particles of a diameter of <10 µm, known as buoyant particles, may travel hundreds of kilometres in the air without sedimenting. According to Ambler and Bain (Ambler & Bain, 1955), the corrosion of metallic surfaces is only caused by salt particles and saline drops of a size of more than 10 µm. Given that these particles remain for just a short time in the atmosphere, corrosion completely loses its marine character just a few hundred metres inland.

However, the distance from the sea is not in itself always the only determining factor for the corrosion rate, which also depends on the topographic and orographic features of the land and on the intensity and direction of prevailing winds, etc.

Abnormally high salinity levels are sometimes recorded as a result of storms, which in just a few hours can deposit larger amounts of salt than the normal wind regime during an entire month.

However, a higher wind speed does not always mean an increase in salinity, which is ultimately dependent on the wind direction. In fact, an increase in the wind speed can even cut the amount of pollution by purifying the atmosphere. This naturally depends on the location of the site in relation to the sea and on the direction and type of the winds blowing at any given time.

Although in principle it would seem reasonable to assume that the presence of marine aerosol in coastal regions would be governed by the speed, direction and duration of marine winds (those proceeding from the sea), the topography and orography of the land and the general wind regime of the local area can also lead continental winds to influence salinity values. This has been shown in a study by the Russian Academy of Sciences (Strekalov & Panchenko, 1994; Strekalov, 1988), in which the authors report observations made over long time periods in Murmansk and Vladivostok, reaching the conclusion that in both areas the transportation of chlorides depended on the average speed of total winds (marine + continental) and on the product of the wind speed by its duration ("wind strength").

Thus, it was of practical interest to quantify atmospheric salinity at Vandellós I nuclear power plant site and its effect on the metallic corrosion process. Specific research work has been carried out in this coastal area of Tarragona (Spain) with the dual aim of determining: a) the influence of atmospheric salinity on metallic corrosion at this location; and b) the influence of winds on the recorded salinity values.

2.1. Effect of atmospheric salinity on metallic corrosion

2.1.1. Experimental

The study has been carried out in three open-air corrosion testing stations located at different distances from the shoreline (Figure 2) (B Chico et al., 1997). Use has preferentially been made of CLIMAT specimens. The CLIMAT test (Classification of Industrial and Marine Atmospheres), also known as the "wire on bolt" technique, is a method for determining the corrosivity of an atmosphere. This procedure was first used in the United States by Bell Telephone Laboratories (Compton et al., 1955) to assess the possible galvanic effects of bimetallic unions in the atmosphere. The technique was subsequently developed by the company Alcan (Doyle & Wright, 1969) to assess the suitability of steel core reinforced aluminium conducting cables for electricity transmission lines. Godard, Doyle et al. (Doyle & Wright, 1969; Godard, 1963; Doyle & Godard, 1963; Doyle & Godard, 1969; Doyle & Wright, 1971) are the researchers who have most widely applied this technique.

The CLIMAT test is a simple and economical method that yields reliable results in a short time (three month periods). This technique assesses the mass loss experienced by a wire wound strongly round the thread of a bolt which behaves cathodically in relation to the wire.

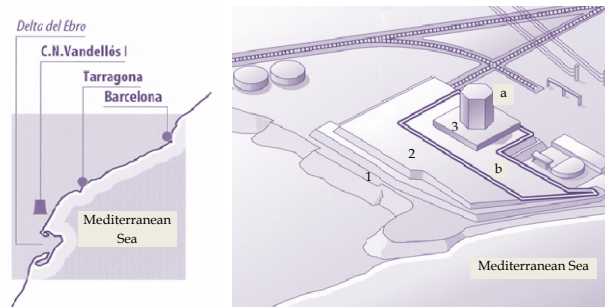


Fig. 2. Sketch with location (points 1 to 3) of corrosion stations

Figure 3 shows a set of the specimens used in the CLIMAT test. Four different types of specimens were tested: Al/Fe, Al/Cu, Al/PVC and Al (spiral). Standard dimensions and materials were used (Morcillo & Feliu, 1977) in order to allow comparison with the results obtained in previous studies and by other researchers.



Fig.3. View of a corrosion station (and corrosion samples) equipped with devices for recording meteorological (wind speed and direction, temperature and relative humidity) and pollution (salinity and SO_2) parameters

Each series of specimens was exposed for three months, after which they were withdrawn and replaced by a fresh series. In total four consecutive testing periods were evaluated. At the end of the test the wire was unwound from the bolt and the corrosion products were removed from the wire using specific solutions (ISO 9226, 1992), calculating the mass loss (ISO 8407, 1991) expressed as a percentage of the initial mass.

Together with the CLIMAT specimens, flat carbon steel and galvanised steel specimens (Fig. 3) were also exposed in the testing stations for a one year period.

In order to determine the aggressivity of the different atmospheres the following meteorological and pollution parameters were recorded: temperature, relative humidity, time of wetness, environmental salinity and SO₂ (Fig. 3). Salinity was determined monthly by the wet candle method (ISO 9225, 1992) and sulphur dioxide by the lead peroxide candle method (BS 1747, 1963). Automatic sensors were used to measure the temperature and relative humidity of the air. The time of wetness (TOW) was determined by calculating the number of hours in which RH ≥ 80% and T > 0°C (ISO 9223, 1992).

2.1.2. Results

Table 1 displays the environmental and corrosion data obtained at the three testing stations.

Corrosion station no.	Environmental data			Corrosion data					
	TDH (hours)	SO ₂ (mg / m ² .day)	Salinity (mg Cl ⁻ / m ² .day)	CLIMAT specimens (%)				Flat specimens	
				Al/spiral	Al/PVC	Al/Fe	Al/Cu	C steel	Galvanised steel
1	2325	7.08	95.56	0.32	0.44	5.94	6.57	29.46	4.72
2	1339	6.93	50.07	0.30	0.32	2.86	3.46	24.35	2.59
3	2462	8.22	26.39	0.22	0.19	1.56	1.86	22.64	1.53

Tabla 1. Mean anual values of environmental and corrosion data obtained in the three testing stations (Fig. 2)

2.1.3. Discussion

2.1.3.1. Damage functions

The environmental and corrosion data obtained with the CLIMAT specimens in the four exposure periods (spring, summer, autumn and winter) was studied in order to establish its significance in the corrosion process.

For this purpose, statistical analysis was performed with the assistance of a specific computer program (BMDP Statistics computer software).

The data was fitted according to the following linear equation:

$$C = a_1 + a_2 T + a_3 RH + a_4 TOW + a_5 Cl + a_6 S \quad (5)$$

where a_i ($i = 1$ to 6) are constants, C is aluminium corrosion (%), T is the average temperature ($^{\circ}\text{C}$), TOW is the time of wetness (hours), S is the average SO_2 pollution value ($\text{mg}/\text{m}^2\cdot\text{day}$), and Cl is the average chloride pollution value ($\text{mg}/\text{m}^2\cdot\text{day}$).

The resulting damage functions between corrosion and environmental parameters are shown below, along with their corresponding correlation coefficients (R).

Specimen type	Equation	R	
Al (spiral)	$C = -0.147 + 0.015 T + 0.002 Cl$	0.80	(6)
Al/PVC	$C = 0.097 + 0.003 Cl$	0.82	(7)
Al/Fe	$C = 0.185 + 0.054 Cl$	0.93	(8)
Al/Cu	$C = 0.315 + 0.059 Cl$	0.91	(9)

Salinity is the variable of greatest significance for all types of CLIMAT specimens. Temperature also emerges as a significant variable only in the case of the Al (spiral) specimen.

Since the atmospheres in question are of a pure marine character with practically no SO_2 pollution, it is not surprising that the Al/Cu specimens, which are sensitive to both marine and industrial atmospheres, only reflect the influence of environmental salinity.

Figure 4 shows the relationships encountered between salinity and corrosion of the Al/Fe and Al/Cu CLIMAT specimens and the carbon steel specimens. Since these are pure marine atmospheres, both Al/Fe and Al/Cu CLIMAT specimens are equally valid when it comes to determining the scope of metallic corrosion, thus confirming the observations made by other researchers (Doyle & Wright, 1982).

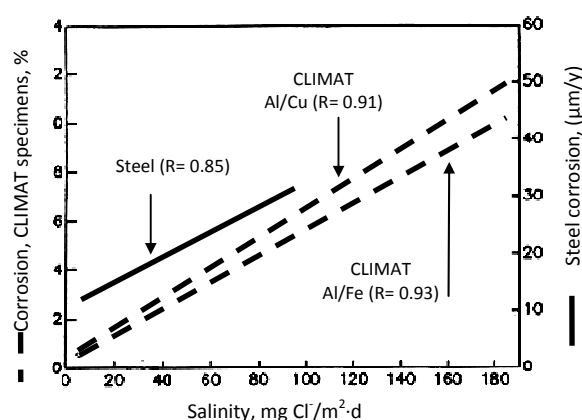


Fig. 4. Relation between the degree of corrosion on Al/Fe and Al/Cu CLIMAT specimens and flat steel specimens and the atmospheric salinity

2.1.3.2. Effect of distance from the sea

In order to obtain a broader view of this aspect, in addition to the corrosion data obtained in the present study consideration has also been made of information reported in the literature, principally from Godard, Doyle and Wright (Doyle & Godard, 1969; Doyle & Wright, 1971; Doyle & Wright, 1982) and the Canadian company ALCAN (Doyle & Wright, 1969). These researchers found that corrosion decreases with the distance from the shoreline following a hyperbolic law:

$$X^{1/3} + Y^{1/3} = K \text{ (constant)} \quad (10)$$

where X is the distance from the shoreline and Y is the marine corrosivity index (MCI). In other words, the variation in the MCI with the distance from the shore is not linear but decreases rapidly in the first few hundred metres and subsequently more gradually; by 1 km inland the value is greatly reduced, and by 2 km inland an asymptotic value is reached.

Furthermore, they note that the higher the MCI at the shoreline, the greater the reach of marine penetration inland.

This function seems to have a certain validity in marine atmospheres, since it is also fulfilled for flat specimens used by other researchers (Ambler & Bain, 1955).

Figure 5 shows the CLIMAT data obtained in this study along with data reported by other researchers (Doyle & Godard, 1969) using CLIMAT specimens on the south-east coast of South Africa (Durban), the north coast of Colombia (Galerazamba), and the east coast of the United States (Kure Beach).

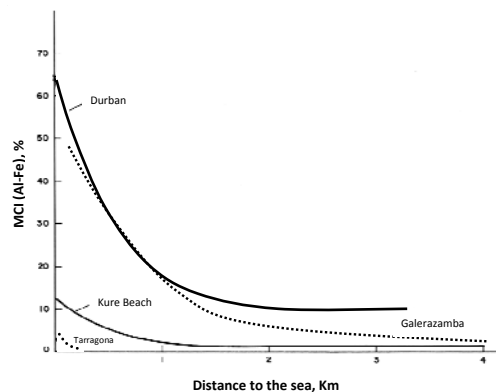


Fig. 5. Relation between the marine corrosivity index (MCI) and the distance from the shoreline

The results obtained in our study also reflect this behaviour, although the K constant values are notably lower (equation 10) due to the lower corrosivity of the atmosphere where the study was carried out.

The higher the K value, the greater the atmospheric corrosion at a given distance from the shoreline and the greater the reach of the marine atmosphere inland.

2.1.4. Conclusions

- Atmospheric salinity is the variable of greatest significance in the metallic corrosion process at Vandellós I nuclear power plant site. A clear linear relationship is established between atmospheric salinity and metallic corrosion, irrespective of the type of corrosivity sensor used (CLIMAT specimen or flat specimen).
- Being a pure marine atmosphere, both Al/Fe and Al/Cu couples can be used as atmospheric salinity and corrosion sensors.
- The decrease in atmospheric salinity inland from the shoreline is exponential, with a notable drop in salinity in the first few hundred metres followed by a more gradual decrease at greater distances inland.

2.2. Influence of the wind regime on atmospheric salinity

2.2.1. Experimental

Information on winds was obtained on the same corrosion station as the salinity data (Figure 3) (Morcillo et al., 2000). Wind speed and direction data was measured with an anemometer and a wind vane and gathered by a 1256 meteodata station (Geónica), recording data every 10 s and calculating averages every 10 min. Atmospheric salinity data was retrieved every 3 months.

2.2.2. Results

Salinity data are displayed in Table 2. Attention is drawn to the high value obtained in the eighth month of testing (March). The monthly distribution of wind frequencies, in hours, for marine winds, *M*, and total winds (marine + continental), *T*, for the different wind speed intervals is shown in Table 3.

2.2.3. Discussion

It seems reasonable to assume that atmospheric salinity will be determined mainly by marine winds, i.e. those blowing from the sea towards the land and thus liable to carry marine aerosol. The testing site is situated on a section of shoreline on the Mediterranean coast, between 40° 57' and 40° 58' latitude, running in SW-NE direction. The range of marine wind directions, including those corresponding to the shoreline, comprises NE, ENE, E, ESE, SE, SSE, S, SSW and SW. The remaining wind directions may be considered continental.

It is interesting to know how each different wind direction contributes to the salinity values recorded in the testing stations.

Month	August	September	October	November	December	January	February	March	April
Salinity (mg Cl/m².day)	27.90	26.37	29.10	10.77	7.31	12.34	8.33	114.47	20.37

Table 2. Chloride pollution of the atmosphere at the nuclear power plant site.

			Velocity interval (m/s)											
			Calm-0.5	0.51-0.75	0.76-1.0	1.1-1.5	1.6-2.0	2.1-3.0	3.1-5.0	5.1-7.0	7.1-10.0	10.1-13.0	13.1-18.0	> 18.1
Frequency distribution of the wind (h)	Aug.	T	1	7	25	98	136	249	150	14	19	7	9	23
		M	1	1	13	46	79	195	112	5	4	3	9	6
	Sep.	T	2	10	24	82	114	171	184	53	42	32	5	1
		M	0	4	6	27	45	95	76	3	0	0	0	0
	Oct.	T	4	5	27	105	113	197	104	10	14	7	0	0
		M	0	1	9	33	39	100	33	3	0	1	0	0
	Nov.	T	5	14	44	170	110	158	113	30	40	27	6	0
		M	0	6	13	47	44	69	41	0	0	0	0	0
	Dec.	T	5	12	48	97	81	117	172	44	106	54	7	0
		M	0	1	9	39	45	55	56	1	0	0	0	0
	Jan.	T	0	3	24	48	62	138	155	65	83	78	63	2
		M	0	0	7	15	39	69	39	0	0	0	0	0
	Feb.	T	4	19	34	83	86	124	152	64	59	27	3	0
		M	1	5	8	32	54	63	44	6	0	0	0	0
	Mar.	T	2	7	36	78	76	136	176	63	55	26	11	0
		M	0	2	12	20	40	81	101	29	6	0	0	0
	Apr.	T	6	14	54	78	102	153	95	23	59	21	10	11
		M	2	3	17	24	62	126	61	3	0	0	7	6

Table 3. Frequency distribution of total winds (marine + continental), T, and marine winds, M, for the exposure period.

Salinity obviously depends not only on the wind speed (v) but also on the number of hours (n) that the wind is blowing in each direction, i.e. the product of $v \times n$, which in meteorology is known as the "wind strength".

Figure 6 illustrates the variation in atmospheric salinity and in marine and total wind strength over time. The variation in total winds (marine + continental) does not coincide with chloride transportation towards the land, since the maximum total wind strength is recorded in the month of January while the maximum salinity corresponds to the month of March. The variation in marine wind strength is that which most closely follows the variation in salinity.

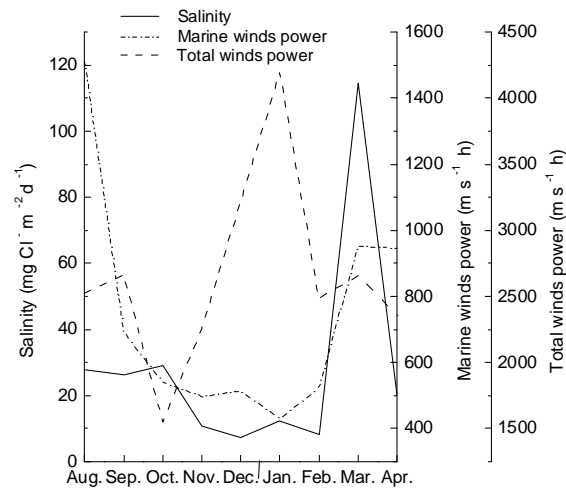


Fig. 6. Relation between atmospheric salinity and wind strength (total and marine)

However, not all the marine wind directions contribute in the same way to the transportation of salinity from the sea towards the land; otherwise, April and August, and not only the month of March, would also present high salinity values.

Plotting the monthly variation in the strength of each marine wind direction shows that the ENE direction (Figure 7) is that which most closely mirrors the variation in salinity data. The marine wind directions that apparently contribute most to the transportation of marine aerosol towards the land may be referred to as 'saline winds'.

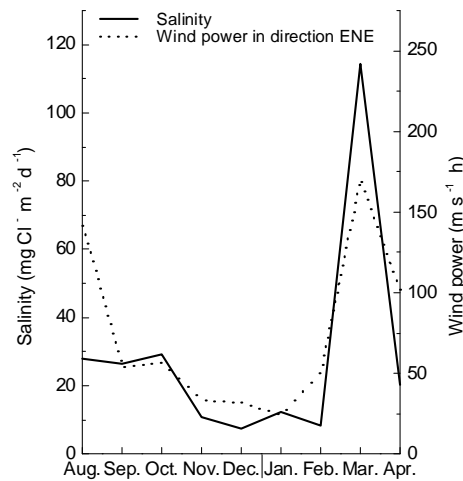


Fig. 7. Relation between atmospheric salinity and wind strength in ENE direction

With regard to a critical wind speed, above which the effect of marine aerosol transportation towards the land is greater, different functions have been tested to relate monthly salinity with the weighted average wind speed. The term weighted average wind speed (v_{mp}) is defined by the expression:

$$v_{mp} = \frac{\sum v_i n_i}{N} \quad (11)$$

where v_i is the mean value of the wind speed range (Table 3) in a given direction, n_i is the number of hours the wind blows in that direction and wind speed range, and N is the total number of hours the wind blows in that direction in all the wind speed ranges.

Of all the tested functions, the polynomial type function is that which provides the best fits, coinciding with the aforementioned studies in Russia (Stekalov & Panchenko, 1994). Figure 8 shows the variation in salinity with the weighted average monthly wind speed for marine winds in ENE direction. For reference purposes, the figure also includes the plot obtained in Vladivostok (Russia) for total winds (marine + continental) according to Stekalov (Stekalov & Panchenko, 1994). As can be seen, the patterns of the three plots are similar. The plot corresponding to winds in the ENE direction seems to indicate a critical speed, close to 3 m/s, above which the transportation of marine aerosol increases considerably.

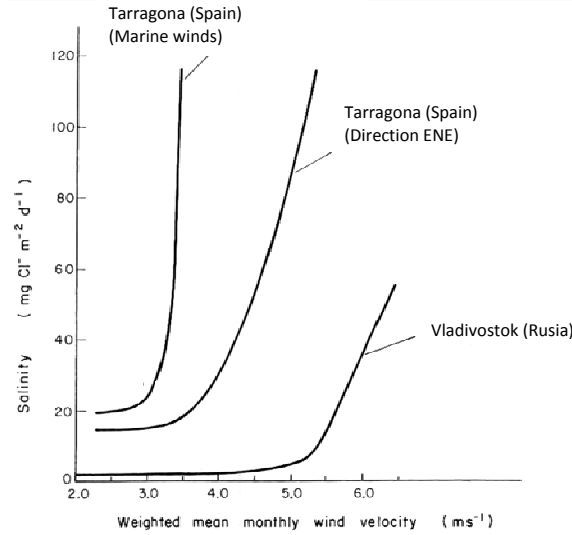


Fig. 8. Relation between atmospheric salinity and weighted mean monthly wind speed for marine winds, winds in ENE direction and total winds (marine + continental), the latter according to Stekalov (Stekalov & Panchenko, 1994)

Another means of establishing the critical speed is by analysing the salinity variation plots for the different months of exposure and the number of hours/month during which the wind speed exceeds a certain value, e.g. 1 m/s, 2 m/s, 3 m/s, etc. Figure 9 shows the plot for wind speeds above 3 m/s corresponding to the ENE direction. As can be seen, the variation in salinity and the number of hours/month during which the wind is blowing in that direction follow very similar patterns.

According to Figure 9, the wind only needs to blow for a relatively short time (27 h/month) at speeds above 3 m/s in a direction with a great influence on the transportation of marine aerosol (ENE direction in this case) for atmospheric salinity to acquire important values.

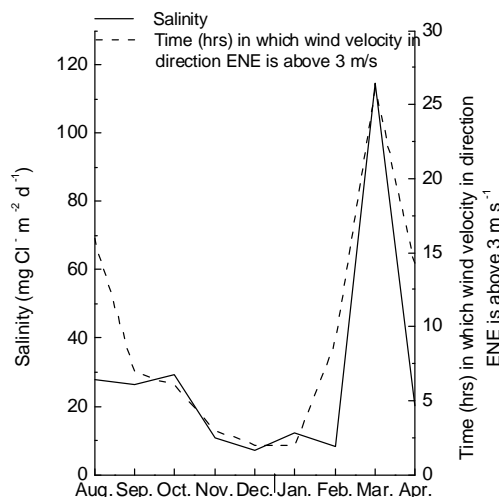


Fig. 9. Relation between atmospheric salinity and number of hours in which the wind speed (v) in ENE direction is above 3 m/s

2.2.4. Conclusions

- This study shows that there are certain marine wind directions (which may be termed 'saline winds') that seem to contribute most to the transportation of marine aerosol from the sea towards the land. At Vandellós I nuclear power plant site, saline winds correspond mainly to the ENE direction.
- There seems to be a critical speed for saline winds above which coastal atmospheric salinity is notably higher. In the present study this critical speed is situated close to 3 m/s.
- The atmospheric salinity of this coastal area seems to depend on the persistence (number of hours) of saline winds above the critical speed.

3. Indoor atmospheric corrosion inside the reactor containment

There follows a description of the experimental technique designed to measure corrosivity inside the reactor containment of the decommissioned Vandellós I nuclear power plant (Otero et al., 2007).

3.1. Constant monitoring of air temperature and relative humidity

The air temperature and relative humidity (RH) are the indoor parameters of greatest influence on the conservation of the reactor containment's internal structures and are constantly monitored.

Temperature measurements are performed using thermocouples located at three levels inside the containment (18, 30 and 49 m) and with different orientations. Figure 10 shows the average temperature values obtained in the upper part of the containment over a two-year period. The temperature remained within the 15°C to 23°C range throughout this period.

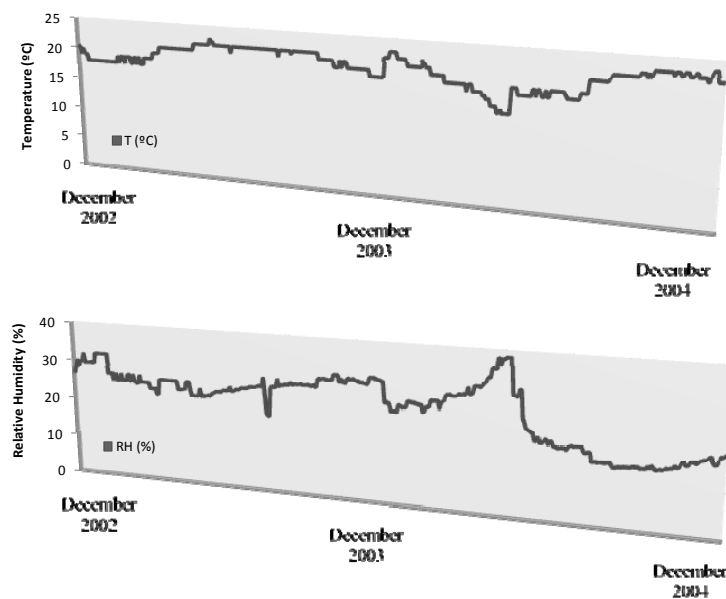


Fig. 10. Average temperature and RH values obtained in the upper part of the reactor containment during a two-year period. An apparent correlation between humidity and temperature (higher temperature = lower humidity) is observed.

RH is measured using a closed circuit system to sample the containment's atmosphere through three extraction tubes located at different heights (high, medium and low), close to the thermocouples, and one return tube. The system is comprised of an extraction pump, filters, connectors for sampling bottles, and an online hygrometer for RH measurements. Figure 10 shows the average RH measured during the same two-year period as the

temperature data, with humidity values in the 15% to 38% RH range. The strength of the radiation field in the test environment is sufficiently low to ignore radiolysis effects.

3.2. Assessment of atmospheric corrosivity inside the reactor containment

The corrosivity of the atmosphere inside the reactor containment is monitored in accordance with ISO 11844-2 (ISO 11844-2, 2005). The techniques selected for this study are "Determination of Corrosion Rate by Mass Changes" (Annex A) and "Determination of Corrosion Rate by Resistance Measurements" (Annex C).

The gravimetric method in Annex A is based on determining the mass change experienced by small rectangular metallic specimens (50 x 10 x 0.5 mm) after different exposure times in the indoor atmosphere. All the tests are carried out in triplicate. Due to the low corrosion rates found in indoor environments, the gravimetric method requires a sensitivity of ± 10 mg/m², and in view of the size of the test specimens a microbalance is used to obtain the necessary sensitivity.

The electrical resistance method described in Annex C of the standard is based on the increase in ohmic resistance that a thin metal film experiences when its cross section decreases. The sensors used in this technique basically consist of two elements, one of which is exposed to the atmosphere (and whose ohmic resistance increases as it corrodes) and another that is isolated from the environment (and whose resistance remains constant). The measurements involve determining the relationship between the two resistance values. Changes in the corrosion rate are shown by variations in the slope of the graph obtained by plotting the results as a function of time. As a result of advances in electronics and data processing, equipment is now available that allows this type of measurement to be carried out in a quick and simple way and which yields data that directly indicates the mean penetration (attack) experienced by the sensor's exposed element due to corrosion.

Determination of corrosion rate by mass changes. For practical purposes, the steels used for the metallic structures located inside the containment have been classified into three groups: a) cold-workable carbon steels; b) low-carbon engineering steels; and c) low-alloy Cr-Mo slow creep-resistant steels. The study tested three representative steels, taking one from each group. The gravimetric specimens (50 x 10 x 0.5 mm) were finished with 320-grade abrasive polishing.

As a result of restrictions on opening the containment and the exceptional safety measures that are adopted in such cases, the withdrawal of mass-change specimens is programmed to occur once every five years.

Determination of corrosion rate by resistance sensor measurements. Determining the corrosion rate by electrical resistance measurements has the advantage of yielding instantaneous data, and the fact that it is not necessary to open the reactor containment to obtain the data. In the present study, electrical resistance measurements are made every three months. Of all the commercially available resistance sensors, an 8-mils (203.2 μ m) thick, flat atmospheric probe

type in UNS K03005¹ pipe grade carbon steel was selected. The measuring equipment used was a CK-4 Corrosometer² by Rohrback Cosasco Systems Inc. (Santa Fe Springs, California). The typical sensitivity of this method is 0.1% of probe life (i.e. its "useful thickness") (ASTM G96-90, 2001). The probe life is normally limited to approximately 50% of the probe element thickness. For the present study, use has been made of steel sensors with a thickness of 8 mils (203.2 μm) and thus a sensitivity of 0.1 μm , in proportion to the sensor thickness.

3.2.1. Experimental setup

Figure 11 shows a general diagram of the experimental setup. The experimental device was installed in the upper part of the reactor containment via three apertures in the ceiling, suspended from a two-disc fixture anchored to the bottom of the seal plugs.

The mass-change specimens and the electrical resistance sensor were placed on a rack which was lowered into the reactor containment through the apertures in the ceiling with the assistance of a manual pulley. The rack suspension cable was fixed to the seal plug and the resistance sensor's connection cable passed through a gland in the centre of the plug. The experimental device was suspended half-way between the containment ceiling and the top of the metallic structures inside the containment. Figure 12 shows a rack being lowered into the containment.

3.2.2. Results

This section presents the corrosion data obtained during the first three years of the study.

3.2.2.1. Measurements obtained with gravimetric specimens

After being carefully withdrawn from the containment, the gravimetric specimens were stored in small boxes containing a desiccant for their transfer to the laboratory. Prior to removal of the corrosion products by pickling, in order to determine the mass losses experienced after three years of exposure inside the containment, the specimens were cleaned carefully with compressed air to remove any dust from their surface and photographs were taken.

A 50 vol% hydrochloric acid (HCl) pickling solution was employed, using hexamethylenetetramine ($\text{C}_6\text{H}_{12}\text{N}_4$) as inhibitor in a proportion of 3.5 g/L (ISO 9226, 1992). The pickling time was 2 min in all cases, with gentle stirring at room temperature, followed by three quick rinses with stirring in distilled water and two quick immersions with stirring

¹ UNS numbers are listed in *Metals and Alloys in the Unified Numbering System*, published by the Society of Automotive Engineers (SAE International) and cosponsored by ASTM International.

² Trade name

in 96% (v/v) ethanol (C_2H_5OH) and absolute ethanol, followed by immediate drying with compressed air. Observation with a binocular microscope, at x20 magnification, confirmed the removal of the corrosion products.

ISO 11844-1 (ISO 11844-1, 2006) expresses mass gain and loss rates in $mg/m^2.y$. In the case of steel, ISO classifies the corrosivity of indoor atmospheres as a function of mass gain and loss into five categories, as shown in Table 4.

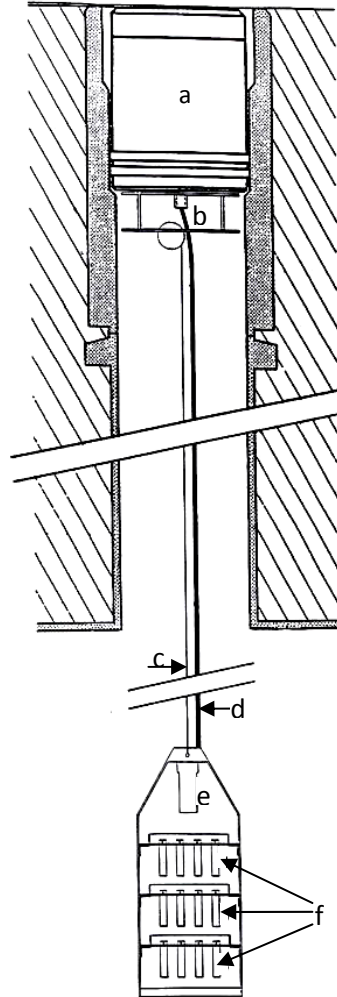


Fig. 11. General setup: (a) seal plug; (b) two-disc fixture anchored to seal plug; (c) braided cable from which rack is suspended; (d) cable connecting resistance sensor to corrosionimeter; (e) electrical resistance sensor; (f) gravimetric specimens.



Fig. 12. Insertion of rack with mass-change specimens and electrical resistance sensor into the reactor containment

Designation	Corrosivity	Mass loss rates (mg/m ² .y)	Mass gain rates (mg/m ² .y)
IC1	Very low	$V_{\text{corr}} \leq 70^{(A)}$	$V_{\text{im}} \leq 70^{(B)}$
IC2	Low	$70 < V_{\text{corr}} \leq 1,000$	$70 < V_{\text{im}} \leq 700$
IC3	Medium	$1,000 < V_{\text{corr}} \leq 10,000$	$700 < V_{\text{im}} \leq 7,000$
IC4	High	$10,000 < V_{\text{corr}} \leq 70,000$	$7,000 < V_{\text{im}} \leq 50,000$
IC5	Very high	$70,000 < V_{\text{corr}} \leq 200,000$	$50,000 < V_{\text{im}} \leq 150,000$

(A): V_{corr} = mass loss rate; (B) V_{im} = mass gain rate

Table 4. ISO classification of the corrosivity of indoor atmospheres as a function of mass loss and gain experienced by carbon steel (gravimetric tests) (ISO 11844-1, 2006)

A more direct description of the attack due to corrosion may be obtained by expressing corrosion behaviour in terms of a "mean penetration rate", in $\mu\text{m}/\text{y}$. This also has the advantage of using the same units as the electrical resistance sensors, thus allowing simple comparison between the results obtained with the two techniques. In order to calculate the corrosion rate in terms of "mean penetration", a value of $7.85 \text{ g}/\text{cm}^3$ was taken as the density of the three types of steel.

The mean corrosion rates obtained by applying the gravimetric technique are set out in Table 5. As can be seen, the mean mass loss rates determined with this method are in the lower limit of the IC2 designation (low corrosivity).

3.2.2.2. Measurements obtained with the electrical resistance sensor

The theoretical sensitivity of this method is a one unit variation in the measurement, which in the case of the installed sensors corresponds to a $0.1 \mu\text{m}$ increase in the mean penetration. However, several factors (ASTM G96-90, 2001) may influence the measurements to an estimated degree of ± 4 units, and thus fluctuations up to this amount should not be interpreted as a reliable indication of corrosion unless a systematic trend is seen in successive measurements.

Table 6 displays the thickness loss values (μm) obtained with the electrical resistance sensors during the first three years of exposure. The fluctuations obtained with each sensor remain within a narrow interval of $\pm 0.2 \mu\text{m}$, which means that corrosion rate estimates cannot be made since the mean penetration experienced by the sensors during this time period is less than their sensitivity threshold.

Group	Type of steel	Containment aperture	Mass loss rates		Mass gain rates
			$\mu\text{m}/\text{y}$	$\text{mg}/\text{m}^2.\text{y}$	$\text{mg}/\text{m}^2.\text{y}$
Cold-workable carbon steels	ASTM C1035	A	0.010	79	26
		B	0.016	128	54
		C	0.004	34	9
		Mean	0.010	80	30
Low-carbon engineering steels	ASTM A516 Grade 60	A	0.015	121	33
		B	0.018	139	54
		C	0.005	41	12
		Mean	0.013	100	33
Low-alloy Cr-Mo slow creep-resistant steels	F-1252	A	0.021	163	49
		B	0.020	158	59
		C	0.003	24	18
		Mean	0.015	115	42

Table 5. Mass loss and gain rates obtained for the three steels below the three containment apertures.

Date	Containment aperture		
	A	B	C
Feb 2002	4.3	3.7	3.9
May 2002	4.3	3.9	3.8
Sept 2002	4.3	3.8	3.9
Jan 2003	4.2	3.8	3.9
Jun 2003	4.2	3.8	4.0
Dec 2003	4.5	3.8	4.1
Dec 2004	4.3	4.0	4.1
Mar 2005	4.3	3.8	3.9

Table 6. Thickness losses in μm obtained with electrical resistance sensors

3.2.3. Discussion

Inspection of the gravimetric specimens upon withdrawal after three years of exposure revealed the presence of corrosion products which in no case fully covered the surface of the specimens. Figure 13 displays an image obtained using scanning electron microscopy (SEM) at $\times 500$ magnification of an area of an F-1252 (UNS G41400) steel specimen with corrosion products that can be seen to follow the direction of the surface finish.

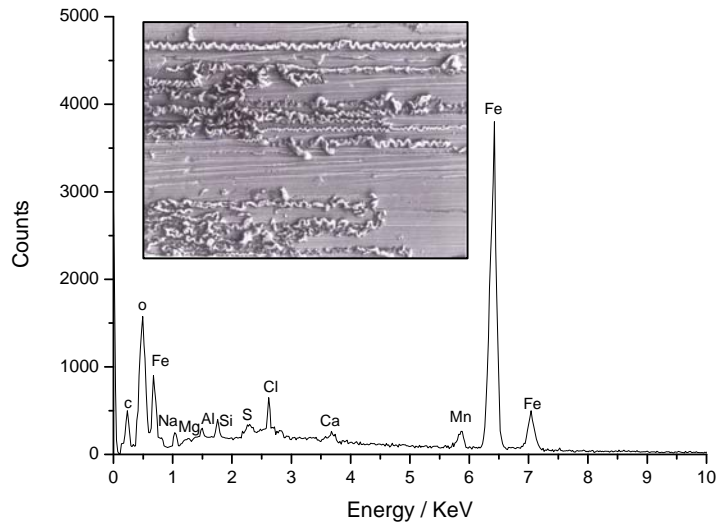


Fig. 13. Appearance of an F-1252 steel specimen in an area with corrosion products (x500) and corresponding EDS microanalysis.

Figure 13 also shows the energy-dispersive spectrum (EDS) obtained by microanalysis of the corrosion product patches formed. Attention is drawn to the presence of Cl in the corrosion products, which indicates the participation of chloride ions in the atmospheric corrosion process. This is not surprising considering the proximity of the power plant to the shoreline. The air is treated before it enters the reactor void by means of filtration of coarse particulates and dehumidification, so only fine to medium-sized salt aerosol particulates are able to enter the reactor containment.

The fact that extremely low corrosion rates are determined, despite the presence of chloride ions, may be attributed to the very low RH (Figure 10) inside the containment, which is below the RH necessary for the formation of moisture films on the metallic surface. Corrosion only takes place by capillary condensation in the grooves on the test specimens, and by the occurrence of differential aeration corrosion processes in these zones. As can be seen in Table 5, the mean values of the mass loss rates obtained were in the interval from 0.010 $\mu\text{m}/\text{y}$ to 0.015 $\mu\text{m}/\text{y}$.

Mean annual carbon steel corrosion rates of 22.6 μm to 29.5 μm were obtained in the different testing stations (see Table 1), 1,500 to 3,000 times greater than the carbon steel corrosion rates recorded inside the reactor containment.

With reference to the results in Table 5, if the mass gain rate (V_{im}) is adopted as a criterion, the indoor atmospheric corrosivity below the three containment apertures (A, B and C) belongs to category IC1 "very low corrosivity" (Table 4). However, according to the mass loss rates (V_{corr}), the indoor atmospheric corrosivity belongs to category IC1 below containment aperture C for all the three studied steels, while the corrosivity below

containment apertures A and B lies within the range of category IC2 "low corrosivity", albeit closer to the lower limit of this category than the upper limit (Table 4).

With regard to the electrical resistance sensors, as has been noted above, the sensors used have a theoretical sensitivity of 0.1 μm average penetration. The small fluctuations in the successive electrical resistance measurements carried out over the three-year period do not allow reliable estimates of the corrosion rate (expressed as mean penetration) and simply indicate that the corrosion experienced by the sensors during this period was lower than or equal to their sensitivity. Since the mean penetration experienced by the sensors during the three years of exposure was less than or equal to 0.1 μm , the annual corrosion rate was less than or equal to 0.03 $\mu\text{m}/\text{y}$.

The gravimetric method confirms the above result, yielding maximum corrosion rates of 0.02 $\mu\text{m}/\text{y}$ (Table 5). This method also indicates a difference in corrosivity between the various sites of the experimental devices: the corrosivity below containment aperture was considerably lower (one order of magnitude less) than below apertures A and B, where the corrosivity was similar. The reason for these differences may lie in small temperature and RH variations between each site.

3.2.4. Conclusions

- The design used to measure the atmospheric corrosion rate inside the reactor containment was shown to work acceptably well, allowing the evaluation of this parameter in accordance with international standards.
- The corrosivity of the atmosphere inside the reactor containment vessel was close to the lower limit of ISO 11844-1 (ISO 11844-1, 2006) corrosivity category IC2 "low corrosivity". As to whether this corrosivity poses a risk to the structures present inside the containment, the very low corrosion rates obtained with both electrical resistance measurements and the gravimetric method indicate that the generalised corrosion experienced by the structures during this period is negligible for practical purposes.

Acknowledgements

The authors wish to express their gratitude to Empresa Nacional de Residuos Radioactivos S.A. (ENRESA) for the funding and the facilities provided for the performance of these studies, and especially to Alejandro Rodríguez for his constant support and guidance.

References

- Ambler, H.R., Bain, A.A.J. (1955). Corrosion of metals in the tropics. *J. Appl. Chem.* **5**, 437-467.
- ASTM G96-90. (2001). "Standard guide for on-line monitoring of corrosion in plant equipment (electrical and electrochemical methods)", West Conshohocken, PA, ASTM International.

- Barton, K. (1976). *Protection against atmospheric corrosion*. Wiley and sons, 0-471-01349-8, London.
- Blanchard, D.C., Woodcock, A.H. (1980). The production, concentration and vertical distribution of the sea-salt aerosol. *Ann. N. Y. Acad. Sci.* **338**, 330-347.
- BMDP Statistics computer software.
- Bonnarens, E., Bragard, A. (1981). *Recherche collective sur la corrosion atmosphérique des aciers*. Report EUR 7400. Commission of the European Communities (Directorate General Information Market and Innovation), Luxembourg.
- BS 1747. (1963). "Methods for the measurement of air pollution. Part. 4. The lead dioxide method." British standards Institution, London.
- Chawla S., Payer, J.H. (1991). Atmospheric corrosion. A comparison of outdoor vs. indoor, *La Metalurgia Italiana*, **84** (2), 135-138.
- Chico, B., Mariaca, L., Otero, E., Morcillo, M. (1997) Evaluación de la corrosión atmosférica en ambientes marinos mediante probetas alambre sobre tornillo. *Afinidad*. LIV, **469**, May-June, 241-245, 0001-9704.
- Compton, K.G., Mendizza, A., Bradley, W.W. (1955). Atmospheric galvanic couple corrosion. *Corrosion*. **11**, 383t-392t, 0010-9312.
- Costa, J.M., Morcillo, M., Feliu, S. (1989). Efecto de los parámetros ambientales en la corrosión. In: *Encyclopedia of environmental control technology*. Cheremisinoff, P.N. (Ed), 197, Gulf Publishing, 0-87201-245-X, Houston.
- Doyle, D.P., Godard, H.P. (1963). A rapid method for determining the corrosivity of the atmosphere at any location. *Nature*. **200** (4912) 1167-1168, 0028-0836.
- Doyle, D.P., Godard, H.P. (1969). Rapid determination of corrosivity of an atmosphere to aluminium. *Proceedings of the 3rd International Congress on Metallic Corrosion*. pp. 429-437. Moscow, MIR Publishers.
- Doyle, D.P., Wright, T.E. (1969). Climat test shows corrosivity. Alcan news. Marzo.
- Doyle, D.P., Wright, T.E. (1971). A rapid method for predicting adequate service lives for overhead conductors in marine atmospheres. The Institute of Electrical and Electronic Engineers (IEEE), Winter Power Meeting, New York, Paper 71. CP 172-PWR.
- Doyle, D.P., Wright, T.E. (1982). Rapid methods for determining atmospheric corrosivity and corrosion resistance. In: *Atmospheric Corrosion*. Ailor, W.H. (Ed), 227-243, Wiley and sons, 0-471-86558-3, New York.

- Feliu, S., Morcillo, M. (1982). Corrosión y protección de los metales en la atmósfera. Bellaterra, S.A., 84-7290-031-2, Barcelona.
- Feliu, S., Morcillo, M., Feliu, S. Jr. (1993). The prediction of atmospheric corrosion from meteorological and pollution parameters - 1. Annual corrosion & - 2. Long-term forecasts. *Corrosion Science*. **34** (3), 403-422
- Godard, H.P. (1963). Galvanic corrosion behaviour of aluminium in the atmosphere. *Materials Protection*. **2** (6) 38-47
- ISO 8407 (1991). Corrosion of metals and alloys. Procedures for removal of corrosion products from corrosion test specimens. Geneva, Switzerland, International Organization for Standardization.
- ISO 9223 (1992). "Corrosion of metals and alloys. Corrosivity of atmospheres. Classification". Geneva, Switzerland, International Organization for Standardization.
- ISO 9225 (1992). "Corrosion of metals and alloys. Corrosivity of atmospheres. Measurement of pollution". Geneva, Switzerland, International Organization for Standardization.
- ISO 9226 (1992). "Corrosion of metals and alloys. Corrosivity of atmospheres. Determination of corrosion rate of standard specimens for the evaluation of corrosivity". Geneva, Switzerland, International Organization for Standardization.
- ISO 11844-2. (2006). "Corrosion of Metals and Alloys - Classification of low corrosivity of indoor atmospheres - Part. 1: Determination and estimation of indoor corrosivity", Geneva, Switzerland, International Organization for Standardization.
- ISO 11844-2. (2005). "Corrosion of Metals and Alloys - Classification of low corrosivity of indoor atmospheres - Part. 2: Determination of corrosion attack in indoor atmospheres", Geneva, Switzerland, International Organization for Standardization.
- Johnson, E., Stanners, J.F. (1981). *The characterisation of corrosion test sites in the community*. Report EUR 7433. Commission of the European Communities (Directorate General Information Market and Innovation), Luxembourg.
- Kucera, V., Mattson, E. (1986). Atmospheric corrosion. In: *Corrosion mechanism*. Mansfeld, F. (Ed.), 211, Marcel Dekker, Inc., 0-8247-7627-S, New York.
- Leygraf, C. Graedel, T.E. (2000). *Atmospheric corrosion*, Wiley-Interscience, 0-471-37219-6, New York.

- Lovett, R.F. (1978). Quantitative measurement of airborne sea-salt in the North Atlantic. *Tellus*. **30**, 358-364.
- Morcillo, M., Feliu, S. (1977). Análisis de la corrosividad atmosférica en España mediante probetas "alambre sobre tornillo". *Rev. Metal Madrid*. **13** (4), 212-222, 0034-8570.
- Morcillo, M., Chico, B., Mariaca, L., Otero, E. (1999). Effect of marine aerosol on atmospheric corrosion. *Mat. Perform.* **38**, 72-77, 0094-1492.
- Morcillo, M., Chico, B., Mariaca, L., Otero, E. (2000). Salinity in marine atmospheric corrosion: its dependence on the wind regime existing in the site. *Corrosion Science*. **42**, 91-104, 0010-938X.
- Otero, E., de la Fuente, D., Chico, B., Madrid, F., Naranjo, V., Morcillo, M. Atmospheric corrosion monitoring inside the reactor vessel of a retired nuclear power plant. *Corrosion*. **63** (6), 591-597, 0010-9312
- Rozenfeld, I.L. (1972). *Atmospheric corrosion of metals*. NACE, Houston, TX.
- Strekalov, P.V. (1988). Wind regimes, chloride aerosol particle sedimentation and atmospheric corrosion of steel and copper. *Protection of metals*. **24** (5), 630-641, 0033-1732.
- Strekalov, P.V., Panchenko, Yu.M. (1994). The Role of marine aerosols in atmospheric corrosion of metals. *Protection of metals*. **30** (3), 254-263, 0033-1732.
- Zeza, F., Macri. (1995). Marine aerosol and stone decay. *The science and the total environment*. **167**, 123-143.